Porphyrazines with Annulated Chalcogen–Containing Heterocycle: Study of Spectral–Luminescent Properties and Quantum–Chemical Calculations of the Excited Electronic States⊗

Konstantin N. Solovyov,[a@] Pavel A. Stuzhin,[b] Valery A. Kuzmitsky,[a,c] Dmitry I. Volkovich,[a] Valery N. Knyukshto,[a] Elena A. Borisevich,[a] and Anwar Ul-Haque[b]

[a] *B. I. Stepanov Institute of Physics, National Academy of Science of Belarus', Pr-t Nezavisimosti, 68, Minsk, 220072, Belarus'*
[b] *Ivanovo State University of Chemical Technology, Friedrich Engels Pr-t, 7, Ivanovo, 153000, Russia*
[c] *Institute for Command-Engineer of the Ministry of Emergency Situations of the Republic of Belarus'*
[@]*Corresponding author E-mail: solovyov@imaph.bas-net.by*

Joint experimental and theoretical study of spectral-luminescent properties and electronic structure of the molecules of new phthalocyanine analogues – derivatives of octaphenylporphyrazine and tetrakis(tert-butyl)phthalocyanine carrying an annulated 1,2,5-thiadiazole or 1,2,5-selenadiazole cycle instead of two phenyl groups or a benzene ring – has been performed. The annulation of a five-membered heterocycle results in bathochromic shifts of the Q_x band and Soret band; the $Q_y - Q_x(S_2 - S_1)$ interval increases and the fluorescence spectra become mirror-symmetrical to the absorption spectra in the region of the $G \rightarrow Q_x$ transition. Replacement of a benzene ring in the tetrakis(tert-butyl)phthalocyanine molecule by the 1,2,5-selenadiazole cycle lowers the fluorescence quantum yield from 0.77 to 0.14 which may be accounted for by the internal heavy-atom effect as well as by intramolecular charge transfer. The fluorescence quantum yield of octaphenylporphyrazine is very low, but for the derivatives it is comparatively high, φ_F=0.06, i.e. the fluorescence is not quenched but enhanced when the heterocycle is annulated. The quantum-chemical calculations of the ground and excited states of the original structures of phthalocyanine, octaphenylporphyrazine, and their derivatives with the annulated thiadiazole cycle have been performed. It is shown that the chalcogen substituted compounds exist as isomers with the NH – NH axis passing through the pyrrole rings devoid of the heterocycle. The calculations based on the INDO/Sm method give reasonable interpretation of the experimental absorption spectra. The description of the properties of the lowest excited Q states is sufficiently good for the phenyl substituted compounds. At the same time, for the Soret band region it is rather difficult to achieve agreement with experiment. Specifically, the energies of the G→B and G→N transitions and the relation between their intensities strongly depends on the values of the dihedral angle made by phenyl ring and the macrocycle.

Keywords: Porphyrazines, 1,2,5-thia- and 1,2,5-selenadiazole, spectral-luminescent properties, quantum-chemical calculations.

Introduction

The substitution of four benzene rings in the phalocyanine molecules can change their physico-chemical properties and even allow to manage them. Annulation of five- and seven-membered heterocycles to the porphyrazine (tetraazaporphine) macrocycle, H_2PA, is an important modification approach in the synthesis of phalocyanine analogues. Study of low-symmetry substituted compounds having from 1 to 3 annulated heterocycles is very important for understanding of the nature of property changes.

In the current paper we report the results of the spectral-luminescence study of new compounds of this type: hexaphenyl(1,2,5-thiadiazolo)porphyrazine (abbreviated as $H_2\{SN_2\}PAPh_6$), its Se-analogue ($H_2\{SeN_2\}PAPh_6$), and also benzo-fused analogue tris(β-*tert*-butylbenzo)(1,2,5-selenadiazolo)porphyrazine ($H_2\{SeN_2\}PA(Bz^tBu)_3$). Here PA is porphyrazine dianion, Ph – phenyl radical, Bz – fused benzene ring, ^{t}Bu - *tert*-butyl group. Chart 1 shows the structural formulae of the studied compounds.

In the tetrapyrrolic macrocyclic systems considered in this study the five-membered heterocycle with two nitrogen and one chalcogen atom (sulfur or selenium) is annulated to the β-pyrrole carbons of one of the pyrrole rings. Molecules of five-membered heterocyclic compounds like pyrrole (C_4NH_5), furane (C_4OH_4), thiophene (C_4SH_4), selenophene (C_4SeH_4) and their azasubstituted analogues form the 6π-electron aromatic systems obeying the Hückel rule (4N+2, N=1), since the imine nitrogen atom, atoms of oxygen, sulfur or selenium deliver to this system pair of electrons from the p_z orbital. As a result, annulation of these heterocycles is similar to annulation of the aromatic six-membered benzene

⊗This paper is dedicated to Professor Boris Dmitrievich Berezin and was originally submitted for the special issue on the occasion of his 80th Birthday (*Macroheterocycles* **2009**, Vol. 2, N. 2).

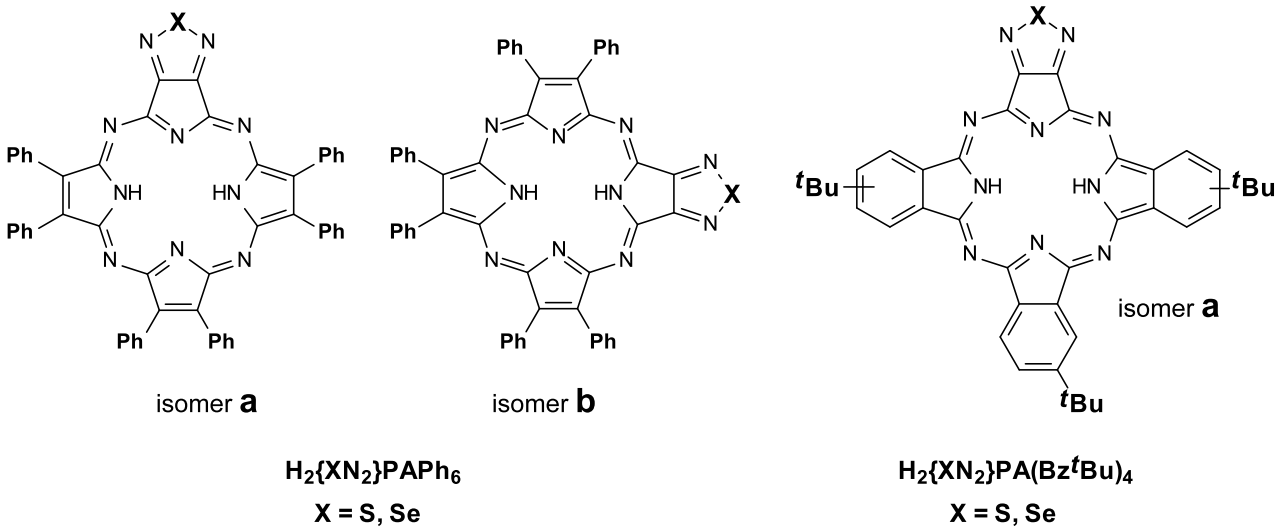

Chart 1. Structural formulae of porphyrazines with annulated chalcogen containing heterocycle.

rings leading to extension of the conjugated π-system. At the same time, the electronic structure and photophysics of the each compound has peculiarities determined by distribution of the electron density in the ground and excited states of the molecule.

Since our goal is the revealing of the nature of spectral changes upon annulation of heterocycle, we analyse and compare the electronic structure and spectral features in the selected pairs of molecules. The results of spectral luminescence study obtained for $H_2\{SN_2\}$-$PAPh_6$ and $H_2\{SeN_2\}PAPh_6$ are compared with the data on octaphenylporphyrazine (H_2PAPh_8), and results for $H_2\{SeN_2\}PA(Bz^tBu)_3$ – with the data for the corresponding phthalocyanine, $H_2PA(Bz^tBu)_4$ ($H_2Pc \equiv H_2PABz_4$). For deeper interpretation of the experimental results we have also made quantum-chemical calculations of the ground and excited states of H_2PAPh_8, $H_2\{SN_2\}PAPh_6$, H_2Pc and $H_2\{SN_2\}PABz_3$.

Materials and Methods

Synthesis of $H_2\{SN_2\}PAPh_6$ and $H_2\{SeN_2\}PAPh_6$ was conducted as described earlier.[1] During chromatographic isolation of these compounds the symmetrical porphyrazine H_2PAPh_8 was obtained as by-product. Its spectral properties are identical with the product obtained following the original Linstead procedure.[2]

Synthesis of $H_2\{SeN_2\}PA(Bz^tBu)_3$ is similar to that of the S-analogue $H_2\{SN_2\}PA(Bz^tBu)_3$ described earlier.[3] Template condensation of 1,2,5-selenadiazole-3,4-dicarbodinitrile (0.09 g, 0.5 mmol) and 4-*tert*-butylphthalodinitrile (0.28 g, 1.5 mmol) was conducted in a solution of magnesium butoxide (from 0.1 g, 4 mmol of magnesium) in dry *n*-butanol under reflux for 5 h. After evaporation of the solvent the residue was washed with 50% aqueous acetic acid (10 ml), then with water, dried, dissolved in CH_2Cl_2 and chromatographed on alumina. The Mg^{II} complex $Mg\{SeN_2\}PA(Bz^tBu)_3$ which was isolated from the second fraction (MS (Maldi-TOF): *m/z* = 760; calc. for $[M^+]$ – 760.2) was demetallated in a CH_2Cl_2-CF_3COOH mixture (1:1) overnight, and, after evaporation of solvents, the residue was chromatographed on alumina to give 9 mg of $H_2\{SeN_2\}PA(Bz^tBu)_3$ (yield ca. 3 %). UV-vis (CH_2Cl_2) λ_{max} nm (lgε): 597 (4.03), 640 (4.46), 661 (4.43), 708 (4.79). IR (KBr) ν cm^{-1}: 3305 (ν_{NH}), 2958s, 2904m, 2869m, 1616m, 1533w, 1483m, 1394m, 1364m, 1315m, 1257m, 1186w, 1090m, 1010s, 914w, 893w, 832m, 745s, 675m, 617w, 518w, 546w. ^1H NMR (CD_2Cl_2) δ ppm: -2.67 (2H, s, NH), 1.26-1.38 (27H, s, *tert*-Bu), 7.50-9.25 (9H, m, CH_{arom}).

The spectral-luminescent characteristics were measured using the automated spectrometric apparatus, described in details elsewhere.[4] The fluorescence quantum yield (Φ_F) was measured relative to a solution of tetraphenylporphine in toluene for which $\Phi_F = 0.09$ (in the presence of air oxygen).[5] The absorption spectra were recorded on a Varian Cary-500 Scan spectrophotometer. Toluene was used as a solvent at ambient temperature, and for the low-temperature measurements at 77 K we have used the vitrifying mixture diethyl ether – toluene (2:1), abbreviated as ET.

Quantum-chemical calculations of the geometric structure were performed by unrestricted Harthree-Fock method using the AM1 Hamiltonian and MOPAC 6 package.[6] Calculations of the excited electronic states of the molecules were made by INDO/Sm method[7] (modified INDO/S method) using our own program. It should be noted that this new INDO/Sm parametrization was elabotated by us recently specially for calculations of porphyrin type systems. The results of the calculation of the *Q* transitions for the fundamental porphyrin systems such as chlorin, bacteriochlorin, tetrabenzoporphine, tetraazaporphine with this INDO/Sm method differ from the experimental data by ~ 300-700 cm^{-1}, while the error of the standard INDO/S method is not less than 3000 cm^{-1}. Calculations of the electronic states have taken into account ca. 400 singly excited electronic configurations with use of the molecular orbitals obtained in the INDO/Sm procedure.

Spectral-Luminescent Properties

H_2PAPh_8. The electronic absorption spectrum of H_2PAPh_8 is shown in Figure 1 *A* (curve *1*). Comparison with the spectrum of unsubstituted porphyrazine (tetraazaporphine), $H_2PA \equiv H_2TAP$, in chlorobenzene (see ref. [8]) shows, that attachment of eight phenyl groups does not change the general spectral pattern, but leads to considerable bathochromic shift of the long-wave absorption bands Q_1(0-0) and Q_2(0-0): from ~617 to ~668 nm (*i.e.* by ~51 nm or ~1200 cm^{-1}) and from 545 nm to 603 nm (*i.e.* by ~58 nm or ~1800 cm^{-1}), respectively. The Soret band (exactly speaking, its analogue) is shifted bathochromically even stronger: in the λ scale from 333 nm to 369 nm, *i.e.* by 36 nm or 2900 cm^{-1}. One should also note the decrease of the energy gap Q_2–Q_1 ($\Delta E_{Q_2Q_1}$) from 2140 to 1610 cm^{-1}, the growth of the intensity of the diffuse absorption band on the long-wave side of the

Soret band and the broadening of the visible bands, especially of the Q_1(0-0) band. This broadening, is connected, most likely, with fluctuations and torsion movements of phenyl rings, which leads to the disturbance of the system and activation of the low frequency non-planar vibrations in the electronic spectra. The observed bathochromic shift results from destabilisation of the highest occupied a_{1u}-type orbital (notation for the D_{4h} symmetry) due to electron-donating effect of phenyl groups.

The fluorescence spectrum of H_2PAPh_8 is also shown in Figure 1 *A* (curve *2*). It can be seen that mirror symmetry of the absorption and emission spectra is absent, which can be explained by overlap of the Q_2(0-0) band with the vibrational structure of the $G \rightarrow Q_1$ transition. The Stokes shift is relatively large (~13 nm, or ~290 cm^{-1}), and halfwidth of the 0–0-band in fluorescence is larger than of the Q_1(0-0) band. These facts are indicative of structural changes (very likely with appearance of non-planarity) in the singlet excited state $S_1(Q_1)$. The spectral shifts due to octaphenyl substitution (transition from H_2PA to H_2PAPh_8) are comparable, and in the UV region even stronger, than due to extension of the π-conjugated system in the case of symmetrical annulation of four benzene rings, *i.e.* in going from H_2PA to H_2Pc (see [9]). However for H_2Pc, its metal complexes and their close analogues the *Q* bands are narrower and the Stokes shift is very small (~50 cm^{-1}), which are considered as an evidence of the planarity of the molecules.

$H_2\{SN_2\}PAPh_6$ and $H_2\{SeN_2\}PAPh_6$. The absorption spectrum of $H_2\{SN_2\}PAPh_6$ is shown in Figure 1 *B* (curve *1*), together with the fluorescence spectrum (curve *2*). Similar data for $H_2\{SeN_2\}PAPh_6$ are displayed in Figure 1 *C*. The obtained data evidence that substitution of two phenyl rings in the molecule of H_2PAPh_8 by five-membered heterocycle, 1,2,5-thiadiazole or 1,2,5 selenadiazole, leads to

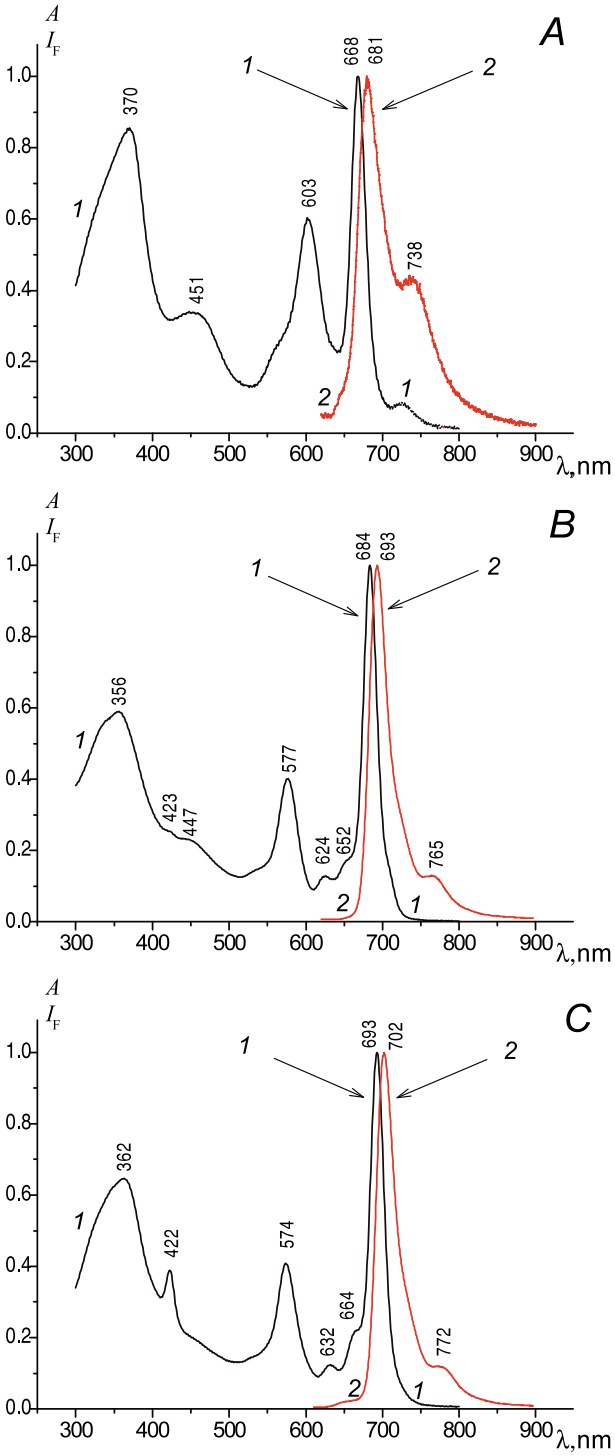

Figure 1. Absorption (*1*) and fluorescence (*2*) spectra of H_2PAPh_8 (*A*, λ_{exc}=602 nm), $H_2\{SN_2\}PAPh_6$ (*B*, λ_{exc}=577 nm) and $H_2\{SeN_2\}$-$PAPh_6$ (*C*, λ_{exc}=574 nm) in toluene at 293 K.

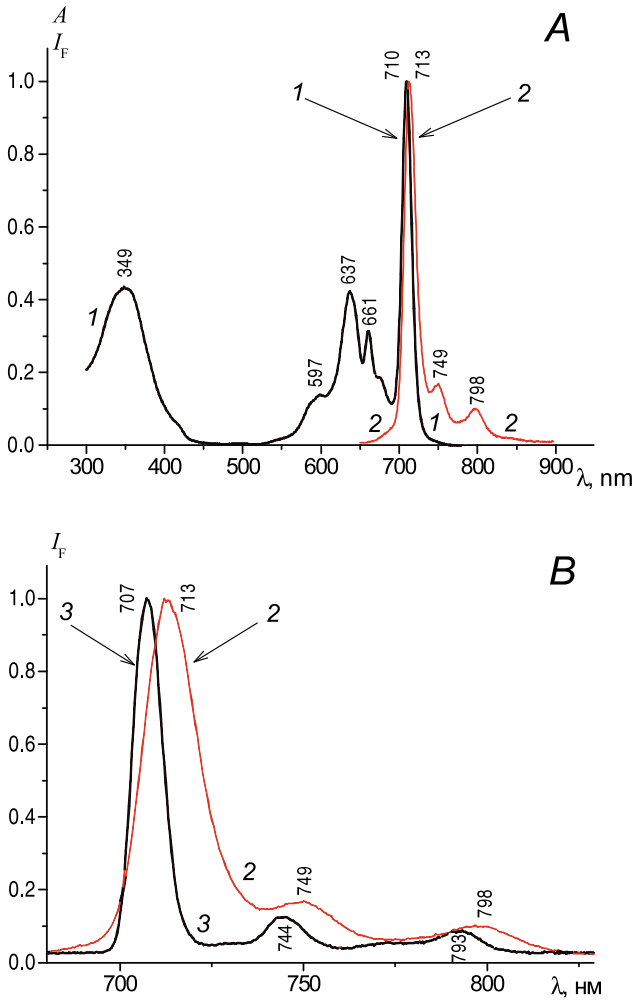

Figure 2. Absorption (*A*, curve 1) and fluorescence spectra (*A* curve 2, *B*, λ_{exc}=350 nm) of $H_2SeN_2(Bz^tBu)_3$ in toluene (*A*; *B*, curve *1*) at 293 K and in the mixture diethyl ether-toluene (2:1) at 77 K (*B*, curve *3*). Curves *A2* and *B2* are identical but have different scale on the λ axis.

the bathochromic shift of the absorption band $Q_1(0–0)$ by 16 and 25 nm (350 cm^{-1} and 540 cm^{-1}), respectively, and also to considerable growth of the energy gap $Q_2–Q_1$ from $\Delta E_{Q_2Q_1}$ = 1610 cm^{-1} to $\Delta E_{Q_2Q_1}$ = 2700 cm^{-1} (S) and 3000 cm^{-1} (Se). The fluorescence spectra are shifted respectively, the Stokes shift and half-width of the 0–0-bands of fluorescence and absorption are somewhat decreased, which might be indicative of increase in the rigidity of the macrocycle. Due to increase of the $Q_2–Q_1$ gap the spectra of fluorescence and absorption become almost mirror-symmetrical. The fluorescence quantum yield in both cases is the same (Φ_F = 0.06).

H_2{SeN_2}PA(Bz^{t}Bu)$_3$. In contrast with the H_2PAPh_8 derivatives, in the absorption spectra of H_2{SeN_2}PA(Bz^{t}Bu)$_3$ (Figure 2, *A*, curve *1*) the $Q_1(0–0)$ is relatively narrow (halfwidth 16 nm, which corresponds the data for $H_2PA(Bz^tBu)_4$[10]). At the same time the 0–0-band of the fluorescence spectrum (Figure 2, *A*,*B*, curve *2*) is slightly broader (halfwidth 20 nm) and the Stokes shift is 18 nm. The latter might evidence about some structural change of the molecule (together with solvate surrounding) in the Q_1 state. At 77 K the fluorescence bands (Figure 2, *B*, curve *3*) as well as absorption bands become narrower and their vibrational structure is better seen. The comparison of the absorption spectrum of H_2{SeN_2}-PA(Bz^{t}Bu)$_3$ (Figure 2, *A*) with the absorption spectrum of $H_2PA(Bz^tBu)_4$[10] shows that substitution of one benzene ring by 1,2,5-selenadiazole moiety leads to a bathochromic shift of the $Q_1(0–0)$ band by ~10 nm. Considerable changes are also observed for H_2{SeN_2}PA(Bz^{t}Bu)$_3$ in the region of the second electronic transition. As a result the $Q_2(0–0)$ band is broadened, its intensity is decreased, and the $Q_2–Q_1$ gap is increased to $\Delta E_{Q_2Q_1}$ = 1620 cm^{-1} from $\Delta E_{Q_2Q_1}$ = 900 cm^{-1} for $H_2PA(Bz^tBu)_4$. These peculiarities of the Q_2 band are evidently connected with action of the vibronic analogue of the Fermi resonance (see ref. [11,12]). In the absorption spectrum of the S-analogue H_2{SN_2}PA(Bz^{t}Bu)$_3$ in dichloromethane the maxima of the Q_1 and Q_2 transitions were observed at 693 and 657 nm with $\Delta E_{Q_2Q_1}$ = 790 cm^{-1}.[3] Therefore upon substitution of S by Se the Q_1 transition is shifted bathochromically by 17 nm (330 cm^{-1}), while the Q_2 transition undergoes a hypsochromical shift by 20 nm (480 cm^{-1}).

The fluorescence quantum yield for H_2{SeN_2}-PA(Bz^{t}Bu)$_3$ Φ_F = 0.14, while for $H_2PA(Bz^tBu)_4$ Φ_F = 0.77.[13] The quenching of the fluorescence might be due to the internal effect of the heavy atom of Se (see ref. [14,15]). The fluorescence quantum yield for the derivatives of H_2PAPh_8 is lower (Φ_F = 0.06), but for H_2PAPh_8 it is even lower, *i.e.* fluorescence is not quenched, but enhanced upon annulation of heterocycle. The reason of the weak fluorescence of H_2PAPh_8 is not clear. It should be noted that the equal values of Φ_F for compounds containing atoms of sulfur (atomic number Z = 16) and selenium (Z = 34) might be explained, at least partly, by the compensation of the heavy atom effect by decrease of the conjugation.

Quantum-Chemical Calculations

Calculated Characteristics of the Excited States

The following characteristics have been determined in calculations of excited singlet states S_k: energies of molecular orbitals φ_i; their delocalization along the molecular fragments $l_A = \sum_{\mu \in A} C_{\mu_i}^2$, where C_{μ_i} – the coefficients of the atomic orbital, A – the number of fragment; characteristics of the S_k states themselves including transition energies from the ground state (E), transition oscillator strengths (f), angle between the transition moment and the x axis, directed along the NH-HN axis, the degree of the electronic density transfer from one fragment to another (L_{AB}), and degree of the localization of excitation on the fragments (L_{AA}) (see ref. [16,17]). For H_2Pc and H_2{SN_2}$PABz_3$ the following fragments have been chosen: 1 – internal 16-membered ring (azacyclopolyene), 2 – all benzene rings together with the C_b-C_b bonds (b indicates β-positions of the pyrrole ring), 3 – annulated heterocycle. In the case of H_2{SN_2}$PAPh_6$ and H_2PAPh_8 the C_b-C_b bonds of the pyrrolic rings which have attached phenyl groups are included in the fragment 1, and fragment 2 includes all phenyl rings. The calculations performed with another atomic distribution, which includes all C_b atoms to the macrocyclic fragment lead to the similar results and are not reported in this paper. Results of calculations are displayed in Figures 4 (MO energies) and 5 (absorption spectra presented as so called "stick diagrams") and in Tables 1–3. Data for H_2PA obtained previously[7] are also presented for comparison.

Geometric Structure of the Ground State

Geometric optimization has shown that the molecule of H_2PAPh_8 has almost planar structure of the macrocycle, and the dihedral angles γ_n between the plane of the phenyl ring n and the plane of the macrocycle are ~40°. Annulation of the 1,2,5-thiadiazole ring instead of two phenyl rings (*i.e.* transition to H_2{SN_2}$PAPh_6$) has only a slight influence on the dihedral angles γ_n. Figure 3 shows the optimized structures of H_2PAPh_8 (*A*) and H_2{SN_2}$PAPh_6$ (*B*) in two projections. For H_2Pc and H_2{SN_2}$PABz_3$ the geometry optimization leads to the planar structure of the molecule. It should be noted that compouds containing one annulated heterocycle can exist as two different NH-isomers (tautomers) – **a** and **b**. In isomers **a** the axis NH–HN goes through pyrrole rings without annulated heterocycle, and in isomers **b** – through pyrrole rings, one of which contains annulated heterocycle. The ground state energy for the isomer **a** is considerably lower than for the isomer **b** for the both investigated compounds H_2{SN_2}$PABz_3$ and H_2{SN_2}$PAPh_6$. Similar behaviour was noticed previously[18] for derivatives of porphine (H_2P) and H_2PA with one annulated 5-membered heterocycle or benzene rings. In the case of H_2{SN_2}$PAPh_6$ the energy of the isomer **b** is higher than for the isomer **a** by 0.25 eV (~2000 cm^{-1} or 6 kcal/mol), and in the case of H_2{SN_2}$PABz_3$ by 0.18 eV (~1500 cm^{-1} or 4 kcal/mol). Since calculations predict the practical absence of the NH-tautomery in the ground state for H_2{SN_2}$PAPh_6$ and H_2{SN_2}$PABz_3$, in the following discussion the results are shown only for the isomers **a**.

Properties of Molecular Orbitals in H_2PA and Its Derivatives

In the case of H_2PA the highest occupied MO (HOMO) φ_{-1} is similar in its structure to the HOMO in the metal complex MPA which has a_{1u} symmetry of the D_{4h} group. It is also similar with one of the quasi-degenerated HOMO ($1a_{1u}$ and

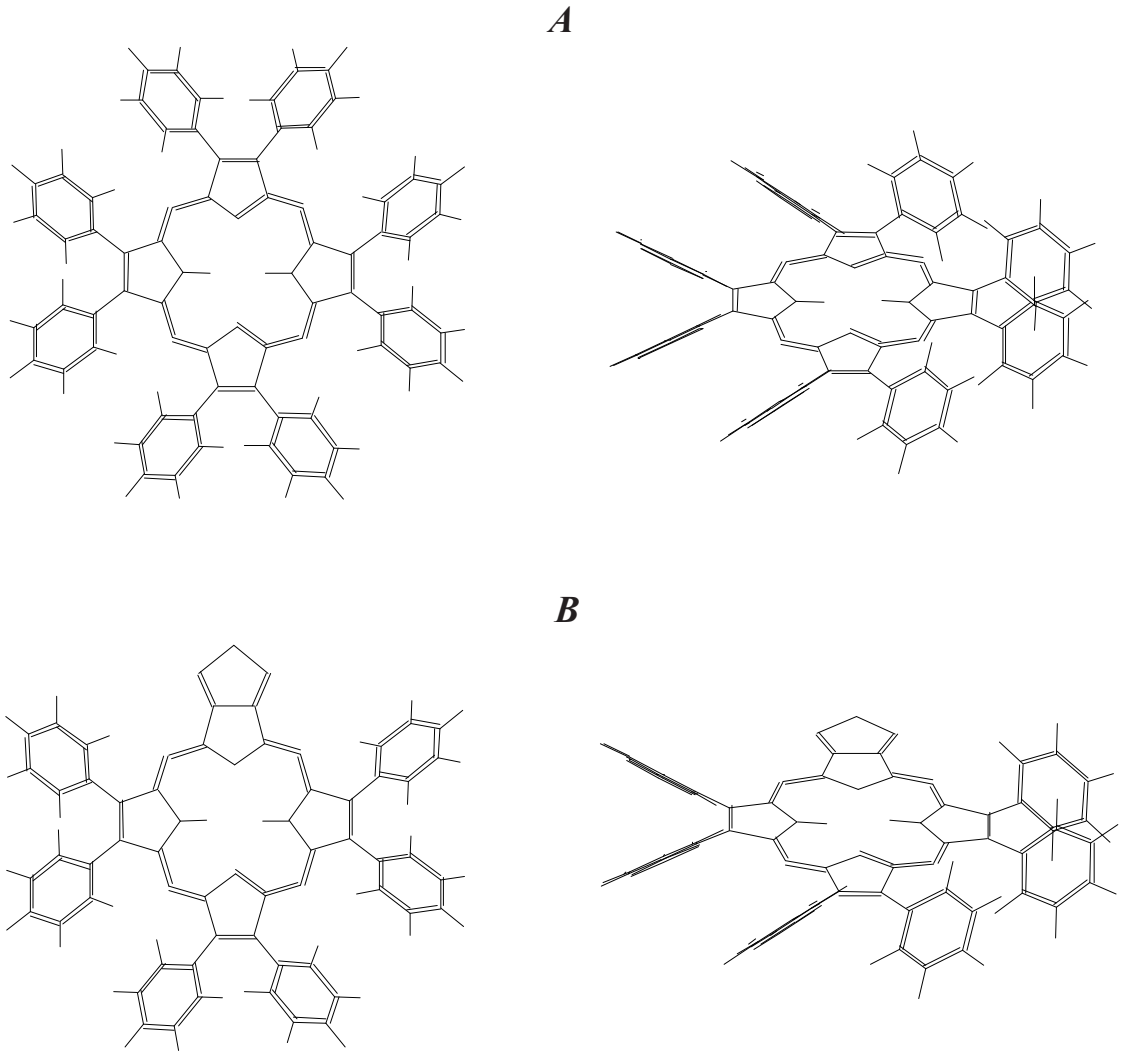

Figure 3. Optimized structures of H_2PAPh_8 (*A*) and isomer **a** for $H_2SN_2PAPh_6$ (*B*).

$3a_{2u}$) of the four-orbital model that adequately describes the lowest excited singlet states in metal porphyrins MP and free-base porphyrins H_2P (symmetry groups D_{4h} and D_{2h}) (see *e.g.* [9,19]). In the four-orbital model, mixing of the $a_{1u}e_g$ and $a_{2u}e_g$ configurations gives two low-energy excited states Q_1 and Q_2, the transitions to which from the ground state *G* have low intensity and determine the absorption spectra of porphyrins in the visible region, and states B_1 and B_2, corresponding to the high intensity Soret band near 400 nm. Here e_g – is the doubly degenerate lowest unoccupied MO (LUMO). The N_1 and N_2 states, transitions to which have intermediate intensity, are located higher. The second HOMO, φ_{-2}, of the four orbital model is $3a_{2u}$, which upon *meso*-azasubstitution (transition from H_2P to H_2PA), becomes lower in energy and mixes with other MO. Because of this and due to changes in the configuration composition the transitions $G\rightarrow B_1$ and $G\rightarrow B_2$ become less intensive, while transitions $G\rightarrow N_1$ и $G\rightarrow N_2$ are intensified. Nevertheless we, as well as the other authors name the intense absorption band in H_2PA and MPA near 330 nm the Soret band (or its analogue).

In the following discussion for notation of the *Q*, *B* and *N* states it is better to use indexes *x* and *y* instead of 1 and 2, since the symmetry of the macrocyclic conjugated system for all considered cases is not lower than C_{2v} and $\pi\rightarrow\pi^*$ transitions should be polarized along the axis *x* (NH-HN) and *y* (perpendicular to *x* in the plane of the molecule). As well as for most derivatives of H_2P, the quantum-chemical calculations for H_2PA give the polarization of the $G\rightarrow Q_1$ transition along the *x* axis, *i.e.* $Q_1 \equiv Q_x$, and $Q_2 \equiv Q_y$.

As can be seen from Figure 4 and Table 1 the introduction of eight phenyl groups increases the energy of the HOMO φ_{-1} «a_{1u}» («» indicates the absence of strict D_{4h} symmetry), while the energy of two LUMOs is only slightly increased. This explains the observed bathochromic shift of the *Q* bands in H_2PAPh_8 as compared to H_2PA. Figure 4 shows also the energy levels of the lower lying filled MO $\varphi_{-2}\ldots\varphi_{-5}$. It can be seen that upon octaphenyl substitution all of them are destabilized and became closer to each other. Apparently this occurs due to conjugation of the phenyl groups with macrocycle (antibonding). This effect should be responsible for the observed bathochromic shift of the Soret band in the experimental spectra in going from H_2PA to H_2PAPh_8.

Annulation of four benzene rings in going from H_2PA to H_2Pc leads to similar changes in the MO level diagram, but the energy of the HOMO «a_{1u}» is more considerably increased as well as that of the vacant levels φ_1 and φ_2.

Table 1. Energies ε_i of the orbitals φ_i [a] and MO localization on the molecular fragments l_A.[b]

i		ε_i, e*V*	l_1	l_2	l_3	ε_i, e*V*	l_1	l_2	l_3
	H_2PA	H_2PAPh_8 ($\gamma_n \approx 40°$)				H_2PAPh_8 ($\gamma = 60°$)			
3		-1.12	72	28		-0.92	81	19	
2	-2.33	-2.32	90	10		-2.25	94	6	
1	-2.43	-2.37	90	10		-2.31	94	6	
-1	-6.16	-5.95	90	10		-5.95	93	7	
-2	-7.89	-6.77	44	56		-7.07	51	49	
-3	-8.34	-6.82	47	53		-7.10	53	47	
-4	-8.59	-6.96	50	50		-7.20	61	40	
-5		-7.20	34	66		-7.50	37	64	
-6		-8.10	55	45		-8.01	24	76	
-7		-8.17	21	79		-8.04	21	79	
-8		-8.19	16	84		-8.17	58	42	
		$H_2\{SN_2\}PAPh_6$ ($\gamma_n \approx 40°$)				$H_2\{SN_2\}PAPh_6$ ($\gamma = 60°$)			
6		-0.17	32	67	1				
3		-1.52	25	3	73	-1.50	26	2	73
2		-2.37	86	6	8	-2.34	88	4	8
1		-2.63	87	8	5	-2.58	90	5	6
-1		-6.07	87	8	5	-6.08	90	5	5
-2		-6.88	45	55	0	-7.19	51	49	0
-3		-7.04	47	53	0	-7.32	56	44	0
-4		-7.27	33	66	0	-7.59	35	65	0
-5		-8.24	34	66	0	-8.11	21	79	0
-6		-8.27	20	80	0	-8.32	55	45	0
	H_2PA	H_2Pc				$H_2\{SN_2\}PABz_3$			
3		-0.61	41	59		-1.38	27	9	65
2	-2.33	-2.01	70	30		-2.29	69	23	8
1	-2.43	-2.20	71	29		-2.42	74	19	7
-1	-6.16	-5.38	72	28		-5.64	74	21	6
-2	-7.89	-7.76	63	37		-7.99	60	40	0
-3	-8.34	-7.90	28	72		-8.17	25	75	0
-4	-8.59	-8.04	18	82		-8.57	10	89	1

[a] Numeration of φ_i: negative *i* values correspond to the filled MOs and positive to the vacant ones in the ground state.

[b] The following molecular fragments are chosen: 1 – internal 16-membered macrocycle (azacyclopolyene) for H_2Pc and $H_2\{SN_2\}PABz_3$; 24-atomic porphyrazine macrocycle for H_2PAPh_8 and $H_2\{SN_2\}PAPh_6$; 2 – all benzene rings together with the C_b-C_b bonds for H_2Pc and $H_2\{SN_2\}PABz_3$ or all phenyl rings for H_2PAPh_8 and $H_2\{SN_2\}PAPh_6$; 3 – annulated heterocycle for $H_2\{SN_2\}PAPh_6$ and $H_2\{SN_2\}PABz_3$.

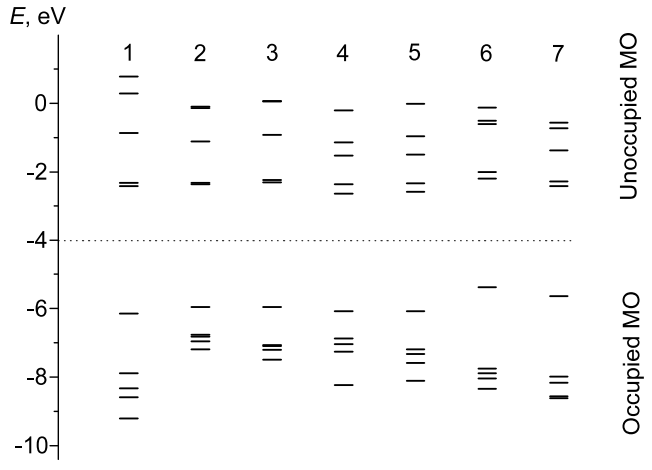

Figure 4. Energies of the highest occupied (HOMO) and lowest unoccupied molecular orbitals (LUMO) for H_2PA and its derivatives: 1 – H_2PA, 2 – H_2PAPh_8 ($\gamma_n \approx 40°$) 3 – H_2PAPh_8 ($\gamma = 60°$), 4 – $H_2\{SN_2\}PAPh_6$ ($\gamma_n \approx 40°$), 5 – $H_2\{SN_2\}PAPh_6$ ($\gamma = 60°$), 6 – H_2Pc, 7 – $H_2\{SN_2\}PABz_3$.

The energy levels of the other filled MOs are destabilized and draw together to a lesser extent than in the case of H_2PAPh_8. Upon annulation of the 1,2,5-thiadiazole ring (instead of the benzene ring or two phenyl groups) the energy of the HOMO «a_{1u}» is only slightly changed. The changes in the MO φ_{-2}…φ_{-5} is stronger – the effect of their rapprochement mentioned above weakens and their energy level distribution becomes closer to the initial level scheme for H_2PA.

Electronic Absorption Spectra

The results of calculations are presented in Figure 5 and Tables 2 and 3. Figure 5 shows also the experimental absorption spectra of H_2PAPh_8, $H_2\{SN_2\}PAPh_6$ and $H_2\{SeN_2\}PA(Bz^tBu)_3$ on the frequency scale.

H_2PAPh_8. For H_2PAPh_8 the calculated energies of the $G \rightarrow Q_x$ and $G \rightarrow Q_y$ transitions (E_{Q_x} = 14900 cm^{-1} and E_{Q_y} = 16400 cm^{-1}) and the energy difference between them ($\Delta E_{Q_yQ_x}$ = 1500 cm^{-1}) are in a good agreement with the experimental values (15000 and 16600 cm^{-1}, $\Delta E_{Q_yQ_x}$ = 1600 cm^{-1}).

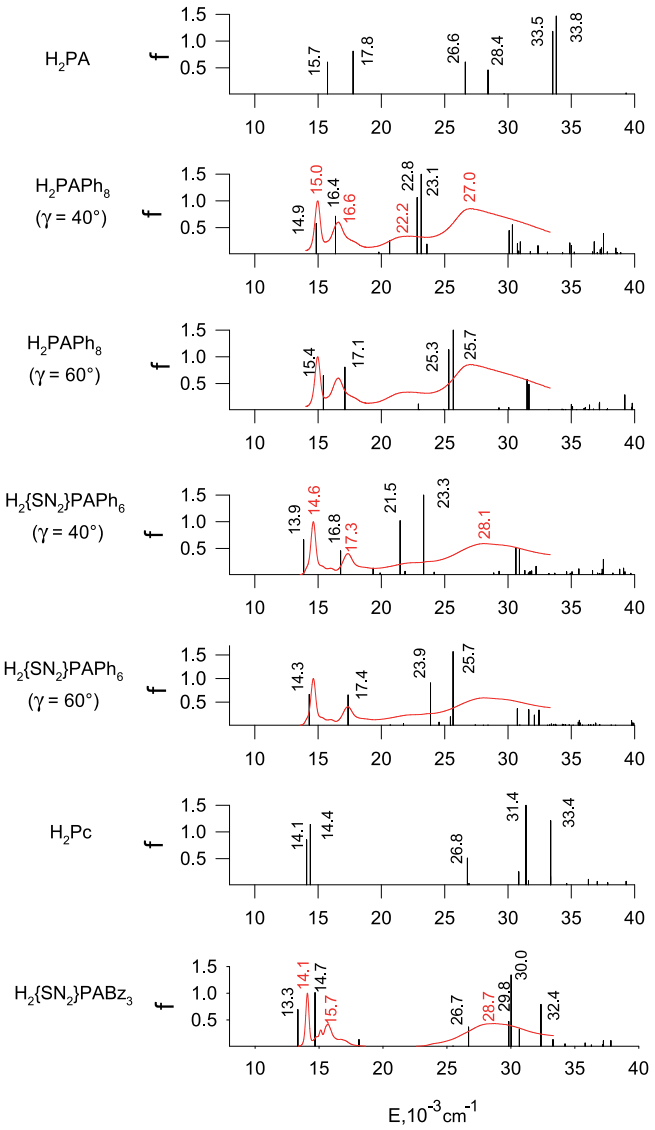

Figure 5. Electronic absorption spectra of H_2PA and its derivatives calculated using the INDO/Sm method. For H_2PAPh_8 and $H_2\{SN_2\}$-$PAPh_6$, and for $H_2\{SeN_2\}PA(Bz^tBu)_3$ the experimental absorption spectra normalized to the maximum of the Q_x band are also shown.

The theoretical and experimental shifts in going from H_2PA to H_2PAPh_8 agree also quite well (Table 3).

In contrast to this the comparison of the calculated data on electronic transitions with the absorption bands of H_2PAPh_8 in the blue and UV regions is difficult. Because of that we have made additional calculations assuming that the energy of the *N* states in the initial calculations was underestimated due to overestimation of the degree of conjugation between the phenyl groups and macrocycle. As a hypothesis we have assumed that for the H_2PAPh_8 molecule in solutions due to intermolecular interactions the dihedral angle between planes of phenyl and macrocycle might be larger than in an isolated molecule ($\gamma_n \approx 40°$). The geometry was then optimized with the fixed values of the dihedral angles $\gamma_n = \gamma$ (*i.e.* all γ_n are equal), and also with rotation of the three selected phenyl groups in the different pyrrole rings, which can model the situation in the solution.

The calculations have shown that upon increase of the dihedral angle γ all transitions are shifted hypsochromically to a different extent. This shift is caused by the increase of the energy gap between LUMO and HOMO. The orbital φ_{-1} «a_{1u}», as well the φ_1 и φ_2 orbitals which have the electronic density localized on the porphyrazine macrocycle are less sensitive to changes of γ values. Therefore the *G*→*Q* transitions are also less sensitive to the changes of γ. Upon increase of the phenyl rotation angle γ the orbitals φ_{-2} to φ_{-5} are considerably lowered (for $\gamma = 60°$ the difference is ≈ 0.3 eV). Approximately the half of the electron density of these orbitals resides on phenyl rings which determines their sensitivity to changes of the γ values. Correspondingly, the energy of the *G*→*N* transitions is changed more considerably when the phenyl rings are rotated. In all calculated variants the changes in the *G*→*N* transition energies are approximately 4.5 times larger than for the *G*→*Q* transitions, which can explain the considerable broadening of the absorption bands in the blue and UV spectral regions. It should be noted that along with the increase of the γ values, some of the MOs which are lower than φ_{-5}, increase their energy, which leads to the change of their relative position. These orbitals are less sensitive to the variation of γ than the φ_{-2}–φ_{-5} orbitals. As a result the change in the energy of the transitions near 30000 cm^{-1} with variation of γ is less, than for the *G*→*N* transitions, although it is 2.5 times larger, than for the *G*→*Q* transitions.

However, the results of calculations with increased values of the dihedral angles γ do not give an unambiguous correspondence between the calculated transition energies and experimental absorption bands in the 22000 – 33000 cm^{-1} region. Below we consider two possible assignments of the calculated and experimental spectra.

The *first variant* of the assignment is based on the direct correlation of the energies and oscillator strengths of the calculated transitions with allowance made for above mentioned factor of the band broadening in the blue and UV spectral regions. In this case the band at 451 nm can be correlated with four transitions two of which are of low intensity (at 22800 and 23100 cm^{-1}), and the band at 370 nm (27030 cm^{-1}) – with transitions of medium intensity at 30100 and 30300 cm^{-1}. Following facts are in support of such assignment. (*i*) For H_2PA the calculated energies of the *N* levels are also higher than in the experiment by ~3000 cm^{-1}. (*ii*) The integral intensity of the broad band at 451 nm is not low. (*iii*) The broadening of the absorption bands in this region correlates with high sensitivity of the *G*→*N* transitions to rotation of phenyl groups. As was shown by calculations with variation of the dihedral angles γ_n, their energy varies from 22000 to 28000 cm^{-1}.

However such assignment provokes some objections. (*i*) The 370 nm band is also broad and its intensity is considerably higher than that of the 451 nm band, *i.e.* most likely the first one is the analogue of the Soret band. (*ii*) Comparison of the experimental absorption spectra of H_2PA and H_2PAPh_8 shows their similarity: introduction of eight phenyl groups leads to the bathochromic shift of all spectral bands. (*iii*) Configuration composition of the states with energy 30100 and 30300 cm^{-1} does not include the electronic configurations related to configurations of the four-orbital model which dominate in the electronic spectra of the H_2P and H_2PA derivatives.

The *second variant* of the assignment assumes that the average value of the dihedral angles γ_n should be larger

Table 2. Characteristics of transitions into the lowest excited states.[a]

$E\cdot10^{-3}$, cm^{-1}	f [b]	Configuration composition of the excitation	L_{11}	L_{12}	L_{13}	L_{21}	L_{22}	L_{23}	L_{31}	L_{32}	L_{33}
		H_2PA									
15.7	0.61 x	$\varphi_{-1}\varphi_1$(-0.93)									
17.8	0.81 y	$\varphi_{-1}\varphi_2$(0.97)									
26.6	0.61 x	$\varphi_{-2}\varphi_2$(-0.85)									
28.4	0.46 y	$\varphi_{-2}\varphi_1$(-0.92)									
33.5	1.18 y	$\varphi_{-4}\varphi_1$(0.92)									
33.8	1.47 x	$\varphi_{-4}\varphi_2$(0.88)									
		H_2PAPh_8 ($\gamma \approx 40°$)									
14.9	0.58 x	$\varphi_{-1}\varphi_1$(-0.93)	79	9		10	1				
16.4	0.71 y	$\varphi_{-1}\varphi_2$(0.95)	77	9		12	2				
20.6	0.25 y	$\varphi_{-2}\varphi_1$(0.89)	45	4		46	4				
22.8	1.06 y	$\varphi_{-4}\varphi_1$(-0.88) $\varphi_{-2}\varphi_1$(-0.32)	38	4		52	5				
23.1	1.63 x	$\varphi_{-4}\varphi_2$(0.76) $\varphi_{-2}\varphi_2$(0.49)	45	6		44	5				
30.1	0.44 y	$\varphi_{-7}\varphi_2$(0.72) $\varphi_{-6}\varphi_1$(0.55)	38	4		51	7				
30.3	0.55 x	$\varphi_{-6}\varphi_2$(-0.74) $\varphi_{-1}\varphi_5$(0.38)	51	17		28	4				
		H_2PAPh_8 ($\gamma = 60°$)									
15.4	0.65 x	$\varphi_{-1}\varphi_1$(-0.94)	87	6		7	1				
17.1	0.81 y	$\varphi_{-1}\varphi_2$(-0.96)	85	6		7	1				
22.9	0.12 y	$\varphi_{-2}\varphi_1$(0.91)	58	3		37	2				
25.3	1.13 y	$\varphi_{-4}\varphi_1$(-0.88) $\varphi_{-2}\varphi_1$(0.33)	44	3		50	3				
25.7	1.91 x	$\varphi_{-4}\varphi_2$(0.79) $\varphi_{-2}\varphi_2$(-0.50)	50	4		43	3				
31.5	0.57 y	$\varphi_{-8}\varphi_1$(-0.91)	62	5		30	3				
31.7	0.48 x	$\varphi_{-8}\varphi_2$(0.87)	42	11		44	3				
		$H_2\{SN_2\}PAPh_6$ ($\gamma \approx 40°$)									
13.9	0.66 x	$\varphi_{-1}\varphi_1$(0.94)	73	7	7	8	1	1	4	0	0
16.8	0.45 y	$\varphi_{-1}\varphi_2$(0.91)	71	6	6	12	1	1	3	0	0
19.3	0.13 y [c]	$\varphi_{-2}\varphi_1$(0.89)	48	4	2	42	4	1	0	0	0
21.5	1.02 y	$\varphi_{-3}\varphi_1$(-0.85) $\varphi_{-1}\varphi_2$(0.34) $\varphi_{-2}\varphi_1$(-0.29)	37	4	2	49	4	2	1	0	0
23.3	1.67 x	$\varphi_{-3}\varphi_2$(-0.83) $\varphi_{-2}\varphi_2$(-0.38)	39	4	4	45	4	4	0	0	0
30.6	0.51 y [c]	$\varphi_{-5}\varphi_1$(-0.63) $\varphi_{-3}\varphi_3$(-0.43)	37	6	10	30	4	14	0	0	0
30.9	0.47 x [c]	$\varphi_{-5}\varphi_2$(0.53) $\varphi_{-1}\varphi_6$(-0.38)	44	14	5	26	4	5	1	1	1
		$H_2\{SN_2\}PAPh_6$ ($\gamma = 60°$)									
14.3	0.66 x	$\varphi_{-1}\varphi_1$(-0.95)	77	4	9	5	0	0	4	0	0
17.4	0.65 y	$\varphi_{-1}\varphi_2$(0.95)	78	4	7	7	0	0	4	0	0
21.7	0.05 y [c]	$\varphi_{-2}\varphi_1$(0.87)	58	3	2	35	2	1	0	0	0
23.9	0.91 y	$\varphi_{-3}\varphi_1$(0.88) $\varphi_{-1}\varphi_2$(-0.25) $\varphi_{-2}\varphi_1$(0.25)	45	2	3	45	2	2	0	0	0
25.7	1.57 x	$\varphi_{-3}\varphi_2$(0.81) $\varphi_{-2}\varphi_2$(0.33)	50	3	4	36	2	3	1	0	0
30.7	0.36 y	$\varphi_{-6}\varphi_1$(0.85) $\varphi_{-3}\varphi_3$(-0.34)	54	3	13	26	2	2	0	0	0
31.6	0.34 x	$\varphi_{-6}\varphi_2$(-0.65) $\varphi_{-8}\varphi_1$(0.44)	34	4	8	41	3	2	3	0	5
		H_2Pc									
14.1	0.85 x	$\varphi_{-1}\varphi_2$(0.96)	51	22		19	9				
14.4	1.14 y	$\varphi_{-1}\varphi_1$(0.99)	49	22		20	9				
26.8	0.51 x	$\varphi_{-2}\varphi_1$(0.92)	39	15		34	12				
30.9	0.25 y	$\varphi_{-2}\varphi_2$(0.95)	39	16		33	13				
31.4	1.75 x	$\varphi_{-4}\varphi_1$(-0.91) $\varphi_{-2}\varphi_1$(0.26)	22	10		51	18				
33.4	1.21 y	$\varphi_{-4}\varphi_2$(-0.89) $\varphi_{-12}\varphi_2$(0.31)	24	8		51	17				
		$H_2\{SN_2\}PABz_3$									
13.3	0.69 x	$\varphi_{-1}\varphi_2$(-0.95)	46	14	14	12	4	3	3	1	1
14.7	1.01 y	$\varphi_{-1}\varphi_1$(0.98)	52	15	6	16	5	2	4	1	0
18.1	0.13 x	$\varphi_{-1}\varphi_3$(0.97)	23	9	44	6	3	11	2	1	3
26.7	0.37 x	$\varphi_{-2}\varphi_1$(-0.82) $\varphi_{-3}\varphi_1$(0.49)	35	10	2	40	10	2	0	0	0
29.8	0.47 x	$\varphi_{-1}\varphi_7$(0.84) $\varphi_{-3}\varphi_1$(0.43)	19	49	1	13	14	1	1	3	0
30.0	1.34 x	$\varphi_{-3}\varphi_1$(-0.70) $\varphi_{-1}\varphi_7$(0.53)	30	25	2	26	11	2	1	1	0
30.7	0.33 y [c]	$\varphi_{-2}\varphi_2$(-0.94)	37	12	4	34	10	2	0	0	0
32.4	0.79 y	$\varphi_{-3}\varphi_2$(0.93)	21	7	3	51	15	3	0	0	0

[a] E – transition energy, f – transition oscillator strength, degree of localization (L_{AA}) and charge transfer (L_{AB}) between molecular fragments upon transition into the excited state as defined in the remark to Table 1. Axis x is directed along the NH–HN axis. Axis y is directed perpendicular to the x axis in the plane of the molecule. The data are given for the states with largest values of f.

[b] Polarization of the transition along x or y axis is indicated.

[c] Values of angles between the x axis and transition moment differs from 0° or 90° in the range from 2° to 8°.

Table 3. Shifts of the Q_x and Q_y levels (ΔE_{Q_x}, ΔE_{Q_y}) and changes in the Q_y–Q_x splitting ($\delta(\Delta E_{Q_yQ_x})$)[a] in the selected molecular pairs (cm^{-1}).

Parameter	calculation $\gamma \approx 40°$	calculation $\gamma = 60°$	experiment[b]	calculation	experiment
	H_2PA – H_2PAPh_8			**H_2PA – H_2Pc**[c]	
ΔE_{Q_x}	-890	-320	-1240	-1640	-1780
ΔE_{Q_y}	-1400	-650	-1770	-3380	-3200
$\delta(\Delta E_{Q_yQ_x})$	-510	-330	-530	-1740	-1420
	H_2PAPh_8 – $H_2\{SN_2\}PAPh_6$			**H_2Pc – $H_2\{SN_2\}PABz_3$**[d]	
ΔE_{Q_x}	-990	-1120	-350 (S) /-540 (Se)	-750	130 (S) /-180 (Se)
ΔE_{Q_y}	410	250	750 (S) / 840 (Se)	300	120 (S) / 550 (Se)
$\delta(\Delta E_{Q_yQ_x})$	1400	1370	1100 (S) /1380 (Se)	1050	-10 (S) / 730 (Se)

[a] $\delta(\Delta E_{Q_yQ_x}) = \Delta E_{Q_{y2}Q_{x2}} - \Delta E_{Q_{y1}Q_{x1}} = (E_{Q_{y2}} - E_{Q_{x2}}) - (E_{Q_{y1}} - E_{Q_{x1}}) = (E_{Q_{y2}} - E_{Q_{y1}}) - (E_{Q_{x2}} - E_{Q_{x1}}) = \Delta E_{Q_y} - \Delta E_{Q_x}$.
[b] Experimental shifts are calculated using the spectral data obtained for H_2PAPh_8, $H_2\{SN_2\}PAPh_6$, $H_2\{SeN_2\}PAPh_6$ and literature data for H_2PA.[8] and H_2Pc.[20]
[c] Experimental shifts are calculated using the spectral data reported for H_2PA[8] and H_2Pc.[20]
[d] Experimental shifts are calculated using the spectral data for *tert*-butyl substituted derivatives – $H_2PA(Bz^tBu)_4$,[10] $H_2\{SN_2\}PA(Bz^tBu)_3$[3] and $H_2\{SeN_2\}PA(Bz^tBu)_3$ (present work).

(by ca 20°) as compared to $\gamma \approx 40°$, and also that the calculated oscillator strengths for the $G \rightarrow B$ transitions are strongly underestimated. The calculations have shown that better correspondence with the experiment in the blue and UV spectral regions is observed at $\gamma = 60°$ and $\gamma = 75°$. At $\gamma = 75°$ the correlation in the transition energy in the Soret band region is better than at $\gamma = 60°$, but the intensity of the $G \rightarrow B$ transitions in the blue region is very low. At such values of the dihedral angle γ the correspondence for the Q bands becomes worse. In Tables 1-3 and in Figure 5 the calculation results are shown for completely optimized geometry and also for the dihedral angle γ fixed at 60° for H_2PAPh_8 and $H_2\{SN_2\}PAPh_6$.

Calculation at $\gamma = 60°$ predicts for H_2PAPh_8 the following sequence of levels: B_y (22900 cm^{-1}), N_y (25300 cm^{-1}) and N_x (25700 cm^{-1}). It can be seen that the accordance for the $G \rightarrow B_y$ transition is very good (λ_{max} = 451 nm corresponds to ν_{max} = 22170 cm^{-1}), but the energy of the N levels is strongly underestimated. It should be noted that the calculated intensity of the $G \rightarrow B$ transitions is low at complete optimization and at all values of γ. It should be admitted that such interpretation leads only to partial agreement with the experiment. This can be due to the unknown real values of γ_n in solution.

$H_2\{SN_2\}PAPh_6$. For this molecule the series of calculations was made with variation of the dihedral angles γ, since the analysis of the spectra in the blue and UV regions has faced with similar difficulties which were observed for H_2PAPh_8 (see above). Tables 1-3 and Figures 4 and 5 present the calculation results for the structure with completely optimized geometry and with the fixed angle $\gamma = 60°$ (similarly to H_2PAPh_8). As compared with H_2PAPh_8 all MO from φ_{-5} to φ_5 are stabilized. For the electronic absorption spectrum in the visible and near UV regions it is important that the LUMO φ_1 is more considerably shifted. The energy gap between MO from φ_{-2} to φ_{-5} is increased. Beside this, despite the decrease of the phenyl groups number from eight to six due to annulation of heterocycle, their contribution in the orbitals from φ_{-5} to φ_5 practically does not change (see Table 1). As a result the variation of the dihedral angles γ_n and γ leads to the similar calculated transition shifts for $H_2\{SN_2\}PAPh_6$ and H_2PAPh_8. The shifts of the MO levels for φ_{-1}, φ_1, φ_2 are similar to the shifts observed upon annulation of one 1,2,5-thiadiazole ring to the H_2PA molecule (transition from H_2PA to $H_2\{SN_2\}PA$).[18] The calculated shifts of the $G \rightarrow Q$ transition energy in the pairs H_2PAPh_8 – $H_2\{SN_2\}$-$PAPh_6$ and H_2PA – $H_2\{SN_2\}PA$, are approximately equal, since the configurational composition of the Q_x and Q_y states in all four molecules are the same (almost "pure" $\varphi_{-1}\varphi_1$ and $\varphi_{-1}\varphi_2$ configurations).

Calculation of the electronic absorption spectrum with full geometry optimization for $H_2\{SN_2\}PAPh_6$ gives relatively good accordance with the experiment in the region of the $G \rightarrow Q$ transitions, which becomes better at $\gamma = 60°$ (see Table 3 and Figure 5). Thus, calculations with $\gamma = 60°$ predict almost pure $\varphi_{-1}\varphi_1$ and $\varphi_{-1}\varphi_2$ transitions at 14300 and 17400 cm^{-1} with $\Delta E_{Q_yQ_x}$ = 3100 cm^{-1}, which is in a good agreement with the experimental values for $H_2\{SN_2\}PAPh_6$ (14600 and 17300 cm^{-1}, $\Delta E_{Q_yQ_x}$ = 2700 cm^{-1}) and $H_2\{SeN_2\}$-$PAPh_6$ (14400 and 17400 cm^{-1}, $\Delta E_{Q_yQ_x}$ = 3000 cm^{-1}).

In contrast to that in the short-wave region we could not reach good agreement between calculation and experiment by variation of the dihedral angles γ or by application of the two assignment approaches considered above for H_2PAPh_8. Calculations with rotation of the phenyl rings in each of three pyrrole fragments also fail to improve agreement with the experiment.

In the region of the $G \rightarrow B$ and $G \rightarrow N$ transitions the calculations of the excited states energies predict the lowering of the B_y and N_y levels for $H_2\{SN_2\}PAPh_6$ as compared to H_2PAPh_8, while the energy of the N_x level remains practically unchanged. This was observed at dihedral angles γ_n, obtained in full geometry optimization and at all varied values of γ. In the experimental absorption spectrum the analogue of the Soret band for $H_2\{SN_2\}PAPh_6$ is shifted hypsochromically to 356 nm (28100 cm^{-1}), the absorption in the blue region becomes weaker and two bands seen at 423 and 447 nm are also hypsochromically shifted.

The shift of the Soret band for $H_2\{SN_2\}PAPh_6$ to higher energy by 1100 cm^{-1} in respect to H_2PAPh_8 observed in the experiment can be explained by the influence on its position of the transitions near 30000 cm^{-1}, which are less sensitive

to variation of the dihedral angles γ_n in the case of $H_2\{SN_2\}$-$PAPh_6$. This band under consideration for phenyl substituted derivatives of H_2PA undoubtly has complicated character, and this question will require more detail investigation.

H_2Pc. The INDOS/m calculations of the H_2Pc molecule with AM1 optimized geometry give the energy of the Q_x transition at 14100 cm^{-1} and Q_y transition at 14390 cm^{-1} ($\Delta E_{Q_yQ_x}$ = 290 cm^{-1}). The mean value of these transitions (14250 cm^{-1}) is in a good agreement with the experimental values (14430 and 15150 cm^{-1}, mean value – 14790 cm^{-1} in dimethylsulfoxide[20]). However, since the absolute polarization of the $G\rightarrow Q_1$ transition in the H_2Pc molecule is unknown, there are some difficulties in interpretation of the results. For the majority of porphyrins it can be considered as well established that the $G\rightarrow Q_1$ transition in the cases of the D_{2h} or C_{2v} symmetry is polarized along the NH–HN axis. In going from H_2PA to H_2Pc, along with the bathochromic shift, the *Q*-bands approach closer each other, and the intensity of the Q_1 band becomes higher than of the Q_2 band (see ref. [9,19]). It cannot be excluded that the transition $G\rightarrow Q_2$ «overrides» the $G\rightarrow Q_1$ transition in degree of energy lowering and becomes the longest wave-length one. However the analysis of our own data on consequitive transition from tetrabenzoporphine (H_2TBP) to H_2Pc by substitution of the methine CH bridges by N-atoms,[21,22] the literature data on absorption spectra of tribenzoporphyrazine[23] and some other facts show, that the Q_1 state of the H_2Pc molecule most likely corresponds to the Q_1 state of the H_2TBP and H_2PA molecules and is the Q_x state. It means that our calculations underestimate the intensity of the $G\rightarrow Q_x$ transition in respect to the $G\rightarrow Q_y$ transition. This occurs, most likely, due to overestimated contribution of the 18-membered azacyclopolyene in the electronic structure of the H_2Pc molecule. Shifts of the *Q*-levels in H_2Pc in respect to H_2PA, which are obtained at such assignment, are given in Table 3.

In the Soret band region the calculations of the H_2Pc spectrum give the electronic transitions similar to the transitions of H_2PA, but with different spectral shifts. The level B_x becomes higher by 200 cm^{-1}, the level B_y – by 2500 cm^{-1}, while the N_x level is lowered by 2400 cm^{-1} and the N_y level by 100 cm^{-1} (the *N* levels are no longer quasi-degenerate). It should be noted that in the absorption spectrum of $H_2PA(Bz^tBu)_4$ in *n*-heptane which is characterized by narrower absorption bands, two components can be seen in the Soret region: shoulder at 358 nm and maximum at 338.5 nm,[10] *i.e.* 27530 and 29840 cm^{-1} (ΔE = 1610 cm^{-1}). For unsubstituted H_2Pc the similar splitting of the Soret band in dimethylsulfoxide (and in dimethylacetamide) is even larger ΔE = 2250 cm^{-1}.[20] In calculations we have obtained 31420 and 33380 cm^{-1} (ΔE = 1960 cm^{-1}) – the correlation with the experiment is not worse that in the case of H_2PA.[7,18] It is important that according to the spectra of magnetic circular dichroism[20] the polarization of the $G\rightarrow N_1$ transition is similar to that of the $G\rightarrow Q_1$ transition and polarization of the $G\rightarrow N_2$ transition is similar with the $G\rightarrow Q_2$ transition. This is in agreement to the results of our calculations.

It is interesting to compare the results of the INDO/Sm calculations for H_2Pc and H_2PA with the data obtained by the currently popular method TDDFT (time-dependent density functional theory) (see *e.g.* [24,25]). In the paper[24] the electronic spectra have been calculated for H_2P, H_2PA, H_2TBP and H_2Pc, only results for the $G\rightarrow Q$ transitions being presented for H_2PA and H_2TBP. The authors[25] have studied the influence of protonation on the electronic structure and electronic spectra of H_2Pc, and non-protonated molecule H_2Pc is considered as an initial structure. These two works report practically the identical data for the *Q*-states of H_2Pc. The comparison of our INDO/Sm results for H_2Pc with the TDDFT results[24,25] shows similarity for the sequence of the Q_x and Q_y levels and configurational composition of these states, and also for the values of the enegy gap $\Delta E_{Q_yQ_x}$. At the same time, the values of the Q_x and Q_y energy levels in our calculations show better agreement with the position of the *Q* bands in solution (see above). Descrepancy with the gas-phase data[26] is almost equal in value but deviation is of the opposite sign – in our work the energy of the Q_x and Q_y transitions is underestimated by ca 500 and 1600 cm^{-1}, while in the TDDFT calculations[24,25] – overestimated by 2000 and 800 cm^{-1}, respectively. For H_2PA the TDDFT method gives even worse agreement with the experiment: E_{Q_x} = 19200 cm^{-1}, E_{Q_y} = 20370 cm^{-1}, while in the experimental spectrum in chlorobenzene E_{Q_x} = 16200 cm^{-1}, E_{Q_x} = 18350 cm^{-1}.[8] Our results obtained for H_2PA by INDO/Sm method are in a suitable agreement: E_{Q_x} = 15700 cm^{-1}, E_{Q_y} = 17800 cm^{-1}.[7]

Between the Soret band and *Q* bands the INDO/Sm calculations predict two transitions (which we denote as B_x и B_y, see above). The TDDFT method gives lower energy and intensity of these transitions as compared with INDO/Sm method. Very likely these two transitions correspond to the weak and diffuse absorption band observed in the spectra of H_2Pc near 450 nm. The configuration composition of the *B* states and their sequence is practically the same in calculations by these two methods.

The calculation results of both methods for the Soret band predict two intense transitions (denoted by us as N_x and N_y) in a similar sequence. The difference is that by TDDFT method several less intensive transitions were obtained with energies close to N_x and N_y. In our calculations these transitions correspond to configurations $\varphi_{-2}\varphi_2$, $\varphi_{-3}\varphi_2$, but their intensity is lower. Both methods overestimate the energy of the N_x and N_y states, but the TDDFT calculations – in a lesser degree. The Soret band maximum of H_2Pc in the gas-phase is located at 29400 cm^{-1},[26] according to TDDFT calculations the mean value of the $G\rightarrow N_x$ and $G\rightarrow N_y$ transition energy is 31000 cm^{-1},[24,25] in our INDO/Sm calculations – 32400 cm^{-1}. Both methods overestimate the relative intensity of the $G\rightarrow N_x$ transition. Therefore we can conclude that calculations of the electronic spectra of H_2Pc by the INDO/Sm and TDDFT methods are in a reasonable agreement with each other and with the experiment.

$H_2\{SN_2\}PABz_3$. Due to the absence of parametrisation for the Se atom in the AM1 and INDO/S methods we have considered the 1,2,5-thiadiazole derivative and accomplished calculations for the species without *tert*-butyl groups $H_2\{SN_2\}PABz_3$. The calculated spectral parameters can be compared with the experimental spectrum of *tert*-butyl substituted species $H_2\{SN_2\}PA(Bz^tBu)_3$ reported earlier[3] and with the spectrum of the Se-analogue $H_2\{SeN_2\}PA(Bz^tBu)_3$ investigated in this work.

Substitution of one benzene ring by 1,2,5-thiadiazole (transition from H_2Pc to $H_2\{SN_2\}PABz_3$) leads to lowering of all orbitals from φ_{-5} to φ_5. For all orbitals from φ_{-2} to φ_2

this stabilization is approximately the same (deviations from the mean value of -0.25 eV do not exceed 0.03 eV). Earlier similar values of these changes have been obtained for the pair monobenzoporphyrazine (H_2MBPA) – mono(1,2,5-thiadiazolo)porphyrazine ($H_2\{SN_2\}$PA).[18]

Calculations of the electronic absorption spectrum of $H_2\{SN_2\}PABz_3$ give the series of levels comparable with the level scheme for H_2Pc. The shifts of levels are from 100 cm^{-1} to 1400 cm^{-1}. Calculation correctly predicts the direction of the shifts for the Q_x and Q_y energy levels and increase of the Q_y–Q_x gap (see Table 3). Calculated energy changes for *Q*-transitions when one benzene ring in H_2Pc is exchanged by 1,2,5-thiadiazole ring in $H_2\{SN_2\}PABz_3$ are close to that obtained for the pair H_2MBPA - $H_2\{SN_2\}$PA.[18] According to calculations the Q_x and Q_y transitions are almost pure ($\varphi_{-1}\varphi_2$ and $\varphi_{-1}\varphi_1$ configurations, respectively). Their calculated energy (E_{Q_x} = 13300 and E_{Q_y} = 14700 cm^{-1}) is somewhat lower and the predicted splitting ($\Delta E_{Q_yQ_x}$ = 1400 cm^{-1}) is larger than in the experimental spectrum of $H_2\{SN_2\}PA(Bz^tBu)_3$ (E_{Q_x} = 14400, E_{Q_y} = 15200 cm^{-1} and $\Delta E_{Q_xQ_x}$ = 800 cm^{-1}[3]). It can be seen from Table 3 that the effect of substitution of one of four benzene rings in phthalocyanine by 1,2,5-thiadiazole ring on the position of the *Q* transitions is poorly described by calculations. The calculations results agree better with the experiment for $H_2\{SeN_2\}PA(Bz^tBu)_3$ (see Figure 5), although the predicted bathochromic shifts are overestimated.

The levels of the states, which can be put in correspondence with the N_x and N_y states of H_2Pc, are lowered by 1400 and 1000 cm^{-1}, respectively. Taking into account such shift, the maximum of the Soret band observed for H_2Pc at 333 nm,[20] should be observed for $H_2\{SN_2\}PABz_3$ at 347 nm. In the experimental spectra the Soret band maximum is observed at 353 nm for $H_2\{SN_2\}(Bz^tBu)_3$[3] and at 349 nm for $H_2\{SeN_2\}(Bz^tBu)_3$ (see Figure 2, *A*).

Calculations show that annulation of the 1,2,5-thiadiazole ring leads to the appearance of new electronic transitions into the states with the predominant contribution of the configurations $\varphi_{-1}\varphi_3$ at 18100 cm^{-1} and $\varphi_{-1}\varphi_7$ at 30000 cm^{-1} (Table 2). These transitions possess characteristic feature of the intramolecular charge transfer (IMCT): the first one contains a large contribution of the electronic density transfer from the macrocycle to five-membered heterocycle, and the second one, from the macrocycle to benzene rings. In the experimental absorption spectrum of $H_2\{SN_2\}(Bz^tBu)_3$ the first of these transitions ma be hidden by the Q_y band and its vibronic satellites, but very likely it can correspond to the additional band which is seen in the spectrum of the Se-analog $H_2\{SeN_2\}(Bz^tBu)_3$ at 661 nm (15100 cm^{-1}).

One can not exclude that in the solution the level of IMCT can be lowered due to fluctuations of solvation interactions, which opens an additional channel for non-radiation deactivation of the S_1 state. This can explain, along with the heavy atom effect, the decrease of the fluorescence quantum yield for $H_2\{SeN_2\}(Bz^tBu)_3$ as compared to H_2Pc. It should be noted that in the case of $H_2\{SN_2\}PAPh_6$ the calculations do not predict the intramolecular charge transfer between the thiadiazole ring and macrocycle in the visible region.

Isomers b. Turning back to the problem of NH-tautomery, we should note that for isomers **b** of the considered compounds with annulated heterocycle the calculation predicts a strong shift of the Q_1 band to the near IR region. This is mainly due to energy lowering of the one component of the strongly split quasi-degenerated LUMO «e_g» (Figure 4). This is connected, in turn, with conjugation of the five-membered cycle with 18-membered azacyclopolyene, which is transfomed to the branched 21-membered cyclopolyene.

Conclusions

The study of the influence of the 1,2,5-thia/selenadiazole annulation on the spectral-luminescent properties of H_2PAPh_8 and $H_2PA(Bz^tBu)_4$ has revealed the correspondence between the initial and modified structures and some peculiarities. Annulation of the five-membered heterocycle leads to a bathochromic shift of the Q_x band and the Soret band, but the difference $\Delta E_{Q_yQ_x}$ is increased and fluorescence spectra become mirror-symmetrical to the absorption spectra in the region of the $G \rightarrow Q_x$ transition. Substitution of one benzene ring in $H_2PA(Bz^tBu)_4$ by 1,2,5-selenadiazole leads to decrease of the fluorescence quantum yield from 0.77 to 0.14, which might be explained by an internal heavy atom effect, and also by contribution of transitions with intramolecular charge transfer. The fluorescence quantum yield for the H_2PAPh_8 derivatives is lower (0.06), but for H_2PAPh_8 it is even less, *i.e.* in this case fluorescence is not quenched but enhanced upon heterocycle annulation. The reason of very weak fluorescence of H_2PAPh_8 is not evident.

Quantum-chemical calculations of the ground and excited electronic states of the basis structures of phthalocyanine and octaphenylporphyrazine and their derivatives with annulated 1,2,5-thiadiazole ring (isomers **a**) has allowed an argumented interpretation of the experimental absorption spectra. Results obtained with the modified parametrization of the INDO/S method – INDO/Sm[7] describe the properties of the low-lying *Q*-states on a semiquantitative level. Effect of 1,2,5-thia/selenadiazole annulation on the energies of the *Q* transitions is reasonably well reproduced for β-phenyl substituted porphyrazines and poorly for benzoannulated species. At the same time in the Soret band region of the phenyl substituted compounds (*B* and *N* transitions) the agreement is less adequate. In particular, the energies of the $G \rightarrow B$ and $G \rightarrow N$ transitions and ratio of their intensities depend strongly on the dihedral angle between phenyl rings and porphyrazine macrocycle. It is shown that the present halcogen-containing compounds considered exist in the form of the isomer **a** with the NH-HN axis passing through the pyrrole rings without fused heterocycle.

Acknowledgements. This study was partly financed by Belarusian Republican Foundation for Fundamental Research (Project F06R-141) and Russian Foundation for Basic Research (Project № 06-03-81022).

References

1. Stuzhin P.A., Pimkov I.V., Ul-Haque A., Ivanova S.S., Popkova I.A., Volkovich D.I., Kuzmitsky V.A., Donzello M.-P. *Zh. Org. Khim*. **2007**, *43*, 1848-1857 (Russ.) [*Russ. J. Org. Chem*. **2007**, *43*, 1854-1863 (Engl.)]

2. Cook A.H., Linstead R.P. *J. Chem. Soc.* **1937**, 929-933.
3. Gaberkorn A.A., Donzello M.-P., Stuzhin P.A. *Zh. Org. Khim.* **2006**, *42*, 946-952 (Russ.) [*Russ. J. Org. Chem*. **2006**, *42*, 929-935 (Engl.)]
4. Zenkevich E.I., Sagun E.I., Knyukshto V.N., Shul'ga A. M., Mironov A.F., Efremova O.A., Bonnett R., Kassem M. *Zh. Prikl. Spektr.* **1996**, *63*, 599-612 (Russ.) [*J. Appl. Spectrosc.* **1996**, 63, 502-513 (Engl.)]
5. Egorova G.D., Knyukshto V.N., Solovyov K.N., Tsvirko M.P. *Opt. Spekrtrosk*. **1980**, *48*, 1101-1109 (Russ.) [*Opt. Spectrosc.* **1980**, *48*, 602-607 (Engl.)]
6. Stewart J.J.P. *MOPAC 6: A General Molecular Orbital Package* (QCPE 445), F.J. Seiler Research Lab., US Air Force Academy: CO 80840 **1990**.
7. Kuzmitsky V.A., Volkovich D.I. *Zh. Prikl. Spektrosk.* **2008**, *75***,** 28-35 (Russ).[*J. Appl. Spectrosc.* **2008,** *75***,** 27-35 (Engl.)]
8. Makarova E.A., Koroleva G.V., Lukyanets E.A. *Zh. Obshch. Khim*. **1999**, *69*, 1356-1361.
9. Kuzmitsky V.A., Solovyov K.N., Tsvirko M.P. In: *Porfiriny: Spektroskopiya, Elektrokhimiya, Primenenie* [*Porphyrins: Spectroscopy, Electrochemistry, Application*] (Enikolopyan N.S., Ed.) Moskva, Nauka, **1987**, 7-126 (Russ.)
10. Mikhalenko S.A., Barkanova S.V., Lebedev O.L., Lukyanets E.A. *Zh. Obshch. Khim*. **1971**, *41*, 2735- 2739.
11. Arabei S.M., Kuzmitsky V.A., Solovyov K.N. *Opt. Spektrosk.* **2007**, *102*, 757-769 (Russ.) [*Opt. Spectrosc.* **2007**, *102*, 692-704 (Engl.)]
12. Arabei S.M., Kuzmitsky V.A, Solovyov K.N. *Chem Phys*. **2008**, *352*, 197-204.
13. Lawrence D.S., Whitten D.G. *Photochem. Photobiol.* **1996**, *64*, 923-935.
14. Mak-Glinn S., Adzumi T., Kinosita M. *Molecular Spectroscopy of Triplet State* Englewood Cliffs, N.J. Prentice-Hall, **1969** [Moskva, Mir, **1972** (Russ. Transl.)]
15. Solovyov K.N., Borisevich E.A. *Usp. Fiz. Nauk* **2005**, *175*, 246-270 (Russ.) [*Physics-Uspekhi* **2005**, *48*, 231-253 (Engl.)]
16. Kuzmitsky V.A. *Issledovanie vozbuzhdennykh elektronnykh sostoyanii dimerov metalloporfirinov metodom SSP MO LKAO* [*Study of the Excited Electronic States of Metallo-porphyrin Dimers Using SCF MO LCAO Method*]. Preprint № 186. Minsk, Institut Fiziki AN BSSR, **1979**. 49 p. (Russ.)
17. Luzanov A.V. Usp. Khim. **1980**, *49*, 2086-2117 (Russ.) [*Rus. Chem. Rev.* **1980**, *49*, 1033 (Engl.)]
18. Volkovich D.I., Kuzmitsky V.A., Stuzhin P.A. *Zh. Prikl. Spektr.* **2008**, *75***,** 606-622 (Russ.) [*J. Appl. Spectrosc.* **2008,** *75***,** 621-636 (Engl.)]
19. Gouterman M.. In: *The Porphyrins* (Dolphin D., Ed). New York, Academic Press, **1978**, Vol. III, 1-165.
20. Martin K.A., Stillman M.J. *Can. J. Chem.* **1979**, *57*, 1111-1113.
21. Sevchenko A.N., Shkirman S.F., Mashenkov V.A., Solovyov K.N. *Dokl. Akad. Nauk SSSR* **1967**, *175*, 545-548 (Russ.) [*Soviet Phys-Dokl*. **1968**, *12*, 710 (Engl.)]
22. Solovyov K.N., Mashenkov V.A., Kachura T.F. *Opt. Spektrosk*. **1969**, *27*, 50-60 (Russ.) [*Opt. Spectrosc*. **1969**, 27, 24-30 (Engl.)]
23. Elvidge J.A., Golden J.H., Linstead R.P. *J. Chem. Soc*. **1957**, 2466-2472.
24. Song Z.-L., Zhang F.-S., Chen X.-Q., Zhao F.-Q. *Acta. Phys.-Chim. Sin*. **2003**, *19*, 130-133.
25. Lu T.-T., Xiang M., Wang H.-L., He T.-J., Chen D.-M. *J. Mol. Struct. (Theochem)* **2008**, *860*, 141-149.
26. Edwards L., Gouterman M. *J. Mol. Spectrosc*., **1970**, *33*, 292-310.

Received 23.07.2009
Accepted 08.02.2010
First published on the web 22.03.2010